

Anisotropic Thermal Diffusivities of Plasma-Sprayed Thermal Barrier Coatings

Megumi Akoshima¹  · Satoru Takahashi²

Received: 12 October 2016 / Accepted: 3 July 2017 / Published online: 15 July 2017
© Springer Science+Business Media, LLC 2017

Abstract Thermal barrier coatings (TBCs) are used to shield the blades of gas turbines from heat and wear. There is a pressing need to evaluate the thermal conductivity of TBCs in the thermal design of advanced gas turbines with high energy efficiency. These TBCs consist of a ceramic-based top coat and a bond coat on a superalloy substrate. Usually, the focus is on the thermal conductivity in the thickness direction of the TBC because heat tends to diffuse from the surface of the top coat to the substrate. However, the in-plane thermal conductivity is also important in the thermal design of gas turbines because the temperature distribution within the turbine cannot be ignored. Accordingly, a method is developed in this study for measuring the in-plane thermal diffusivity of the top coat. Yttria-stabilized zirconia top coats are prepared by thermal spraying under different conditions. The in-plane and cross-plane thermal diffusivities of the top coats are measured by the flash method to investigate the anisotropy of thermal conduction in a TBC. It is found that the in-plane thermal diffusivity is higher than the cross-plane one for each top coat and that the top coats have significantly anisotropic thermal diffusivity. The cross-sectional and in-plane microstructures of the top coats are observed, from which their porosities are evaluated. The thermal diffusivity and its anisotropy are discussed in detail in relation to microstructure and porosity.

Selected paper from Asian Thermophysical Properties Conference.

✉ Megumi Akoshima
m-akoshima@aist.go.jp

¹ National Institute of Advanced Industrial Science and Technology (AIST), 1-1-1 Umezono, Tsukuba, Ibaraki 305-8563, Japan

² Tokyo Metropolitan University, 1-1 Minami-Osawa, Hachioji, Tokyo 192-0397, Japan

Keywords Anisotropy · Flash method · Thermal barrier coating (TBC) · Thermal diffusivity

1 Introduction

The energy efficiency of gas turbines in power plants is expected to improve by operating them at higher than currently used temperatures. The parts of the gas turbine that are exposed to such high temperatures have to be protected from heat, oxidation, and corrosion by applying thermal barrier coatings (TBCs). These are typically two-layer coatings consisting of a metallic bond coating and a ceramic top coating (TC) and tend to be applied by thermal spraying. Each coating layer is several hundreds of microns thick. The TC is expected to play the role of a thermal shield. Many different types of TC have been developed [1], the thermophysical properties of which are important for thermal design. The focus is usually on the thermal conductivity in the thickness direction of a TBC because heat generally diffuses from the surface of the TC to the substrate. The thermal conductivity and/or thermal diffusivity of TBCs has been studied by the flash method using self-standing specimens or layered specimens with a substrate [2–8]. Recently, multilayer models for the flash method were proposed to calculate the thermal conductivity of layered materials as a function of thermal diffusivity, specific heat, and bulk density [4, 7, 9–13], and some studies have applied these models to experimental measurements [4, 7, 8]. The thermal diffusivity of a layer of the layered materials can be calculated from an experimental temperature change curves and a theoretical temperature change curves curve of a multilayer model [4, 7, 9–11, 13] by the least-squares method. The thermal diffusivity can also be estimated from the apparent thermal diffusivity of the layered material obtained using a procedure [8] based on the areal heat diffusion time method [12]. We contributed to the publication of ISO 18555, which is a technical document on estimating the thermal conductivity of each layer of a TBC using a specimen consisting of a TBC and a substrate and using the flash method [14].

However, it has also been pointed out that in-plane thermal conductivity is as important as cross-plane thermal conductivity in the thermal design of advanced gas turbines. This is because there are certain hot spots on a turbine blade [15] and there is the temperature distribution in the turbine which cannot be ignored. In many cases, TBCs are applied by thermal spraying, in which melted or semi-melted materials are sprayed onto a substrate. Because thermally sprayed coatings have a laminate structure that consists of pancake-like particles, the concern is that the thermal conduction of the TC is anisotropic. Currently, no detailed information is available on the anisotropic thermal conduction of the TC in relation to its microstructure, even though such information is expected to be useful for the strict thermal design of gas turbines.

In this study, we develop a method for measuring the in-plane thermal diffusivity of the TC. We use the laser flash method to measure the cross-plane and in-plane thermal diffusivities of self-standing TC specimens formed under different thermal spraying conditions to investigate the anisotropy of thermal conduction in the TC. We use the usual setup of a square-plate specimen for the cross-plane measurement. To measure the in-plane thermal diffusivity, we cut small strips from the square-plate specimen

and bundle them using a ceramic jig which originally designed for this study. We heat one side of the bundle with a pulse laser and measure the temperature change on the other side with an infrared radiometer. By this method, we can obtain the in-plane thermal diffusivity of the TC. We discuss the thermal diffusivities and anisotropy in relation to the TC microstructure.

2 Experimental

Yttria-stabilized zirconia (YSZ) TCs were prepared by thermal spraying under various conditions as summarized in Table 1. They were made from two types of raw powdered ZrO_2 and 7- or 8-mass% Y_2O_3 , namely either fused and crushed powder (F&C) or hollow-sphere powder (HOSP). Air plasma spraying (APS) or water plasma spraying (WPS) was used as the thermal spraying process. The self-standing YSZ specimens were removed from their substrates and bond coats by mechanical and/or chemical processing. Several specimens that were 10 mm square and 1 mm thick were obtained for each spray condition. To compare thermal diffusivities between TCs made by thermal spraying and those made from sintered ceramics, we also prepared specimens of JFCC ZR1 [16] as a typical sintered YSZ ceramic (Table 2).

Cross-sectional and in-plane images of each specimen were observed using an electron microscope. A 1 mm \times 3 mm \times 0.1 mm specimen was cut off from 10 mm square TC. Its surface was locally polished by an ion beam and was observed. The porosity was estimated from the cross-sectional and in-plane images by calculating the areas corresponding to ceramic parts and pores in binarized images. The pores were distinguished by their shape, which varied between lamellar and globular. The total porosity was also estimated by using Archimedes' principle [17].

In the present study, thermal diffusivity measurements were taken by using the flash method at room temperature. The flash method was developed to measure the cross-plane thermal diffusivity of a plate-shaped specimen [18] and has been well studied in relation to, for example, theoretical corrections for heat loss and finite pulse

Table 1 Coating process of various TC specimens

Code	Powder (material component, particle size)	Spray process
YD	ZrO_2 -7-mass%- Y_2O_3 (F&C, 10–45 μ m)	APS
YP1	ZrO_2 -8-mass%- Y_2O_3 (HOSP, 11–125 μ m)	APS
YW	ZrO_2 -8-mass%- Y_2O_3 (F&C, 45–106 μ m)	WPS
YP2	ZrO_2 -8-mass%- Y_2O_3 (HOSP, 11–106 μ m) + 10 % Polyester (45–125 μ m)	APS + annealing (1073 K \times 2 h in air)

Table 2 Sintered YSZ ceramic specimen

Code	Material component	Synthesis process
YSZ	ZrO_2 -3-mol%- Y_2O_3	HIP

width [19–23], multilayer models [4, 7–13], and practical use in applications [24]. Currently popular are xenon laser flash systems for measuring thermal diffusivity along the cross plane of plate-shaped specimens, and these are often used to characterize TBCs.

We measured the cross-plane thermal diffusivity of each of our TCs using $10\text{ mm} \times 10\text{ mm} \times 1\text{ mm}$ specimens. One of the $10\text{ mm} \times 10\text{ mm}$ surfaces of the specimen was heated by a uniform laser beam, and the temperature change on the opposite surface was detected by an infrared radiometer according to the usual setup of the laser flash method as shown in Fig. 1(a). The thermal diffusivity for each temperature time series (temperature change curve) was obtained by an equiareal method [25]. For this, we used a theoretical curve based on the analysis of Cape and Lehman [21] corrected by Josell et al. [22], which considers the effect of radiative heat loss. The theoretical curve was useful for measuring the low thermal diffusivity materials such as the TCs because the effect of heat loss cannot be ignored.

In contrast, the in-plane thermal diffusivity was measured using bundled strips. Each strip measuring $10\text{ mm} \times (2\text{--}3)\text{ mm} \times 1\text{ mm}$ was cut from a TC plate (Fig. 1(b)), and together they were bundled into an original designed jig made of YSZ, as shown in Fig. 1(c). The sides of the jig kept the specimen bundle from twisting. Both ends of the bundle were polished to give a uniform thickness (the width of the strip-shaped specimen). The one end was heated by a pulsed laser beam with the jig masked, and the temperature change at the other end was detected by an infrared radiometer. This way, the in-plane thermal diffusivity was measured successfully as it was for the cross-plane direction. We developed this procedure for two reasons: We seek to make direct comparisons between cross- and in-plane thermal diffusivities measured by the same method, and the TC thermal diffusivity is very low. Although certain practical attachments are commercially available for measuring in-plane thermal diffusivity based on radial heat flow [24], they are better suited to uniform materials with high thermal diffusivity.

In the present study, the heated and measured surfaces of the specimens were coated with Au-sputtered thin films sprayed with carbon to absorb the pulsed laser beam and stop it from penetrating the infrared radiometer.

3 Results and Discussion

Figure 2 shows microstructural images of the TCs used in this study, where (a)–(d) and (e)–(h) show the cross-plane and in-plane microstructures, respectively. The microstructure differs according to the plasma spraying conditions. Sample YD was the most dense among these TCs, with what seems to be an almost isotropic structure (Fig. 2(a) and (e)). Sample YP1 shows some small pores and linear pores (cracks). Sample YW shows a characteristic microstructure with long linear pores in the cross-plane image. Sample YP2 has large globular pores and many linear pores. Note that the all cross-plane images show a characteristic laminated microstructure. Many of the linear pores in the cross-plane images can be considered as lamellar pores. In the all in-plane images, a microstructure associated with spread particles and fused particles is observed.

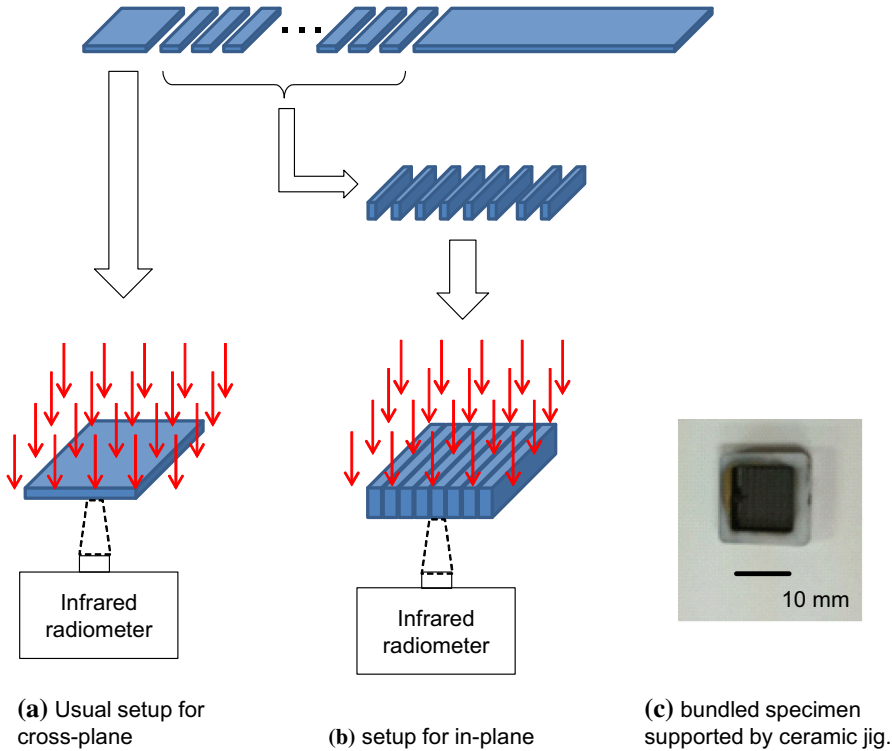


Fig. 1 Principle of cross-plane and in-plane thermal diffusivity measurement by the flash method

We used image analysis to estimate quantitatively the total porosity, the porosity of the globular pores, and the porosity of the linear pores, as shown in Fig. 3. More than five cross-sectional images per specimen were observed and binarized. The porosity was calculated from the relative areas of white and black in the binarized images. Globular pores and line cracks were distinguished according to their circularity [26], which is defined as

$$CI = 4\pi \frac{A}{L^2},$$

where A is the pore area and L is the pore perimeter; CI values of 1 and 0 correspond to a perfect circle and a line, respectively.

Here, linear pores are defined as those satisfying both $0 \leq CI < 0.3$ and $0 \leq A < 1000 \mu\text{m}^2$. The total porosities in the cross- and in-plane views are almost the same in the YD and YP1 samples, whereas in the YW and YP2 samples the cross-plane total porosity is greater than that of the in-plane. The ratio of globular porosity to linear porosity in the YP2 sample differs between the cross- and in-plane views, whereas this ratio is similar between views for each of the YD, YP1, and YW samples. For confirmation, we used Archimedes' principle to estimate the total porosity [17]: That estimated by cross-sectional image was roughly 5% smaller than that measured by Archimedes' principle for all specimens. This seems reasonable, because it is some-

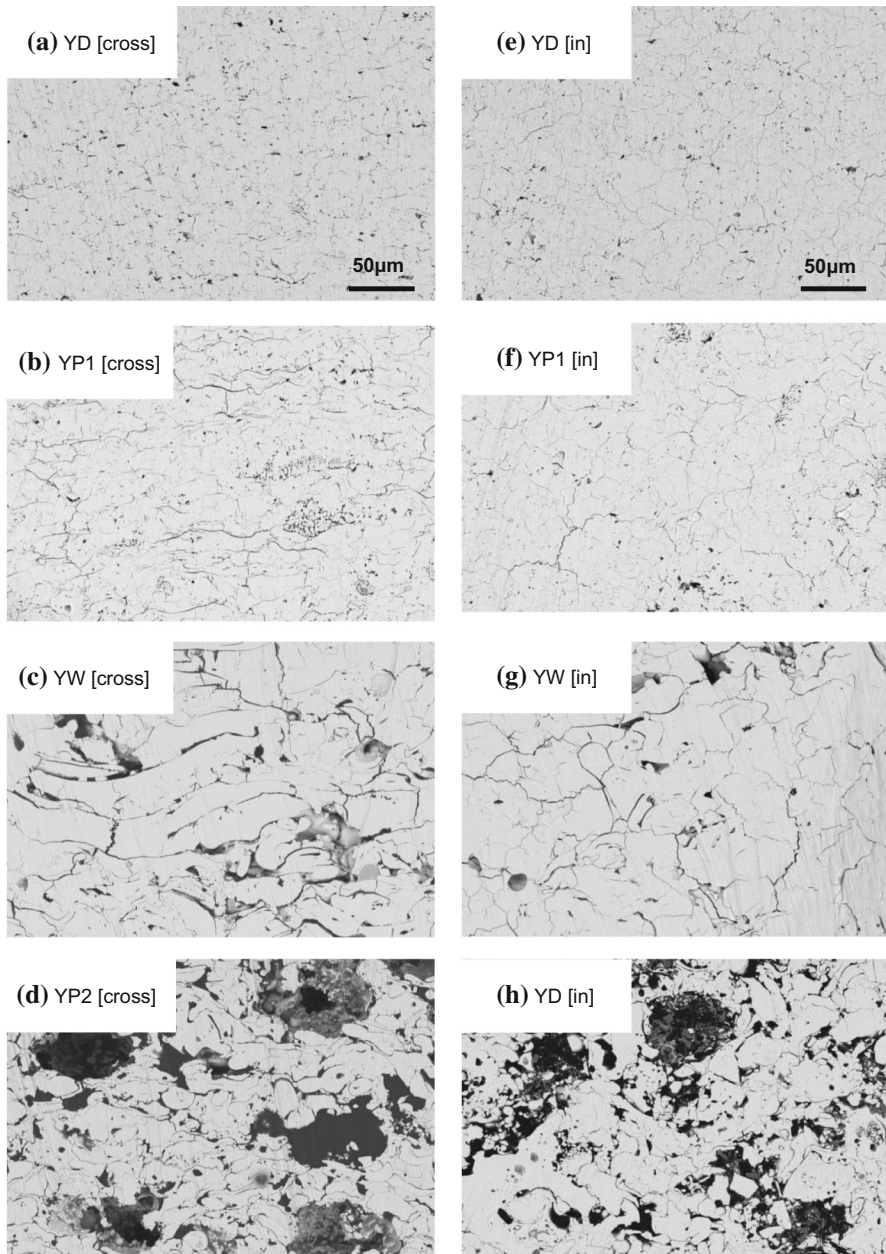


Fig. 2 Microstructural images of various TCs: (a)–(d) cross plane; (e)–(h) in plane

times difficult to detect very tiny cracks with image analysis whereas Archimedes' principle is sensitive to them. Hence, we consider that this comparison validates the estimation of porosity from cross-sectional images.

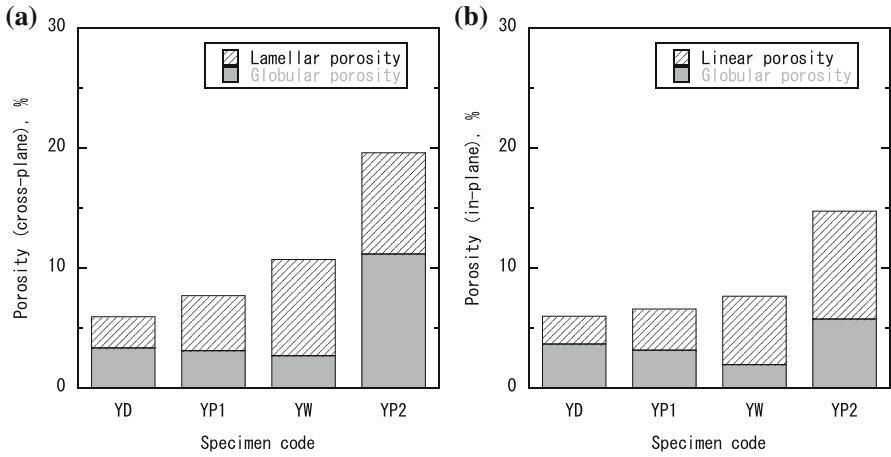


Fig. 3 Porosities of various TCs: (a) cross plane; (b) in plane

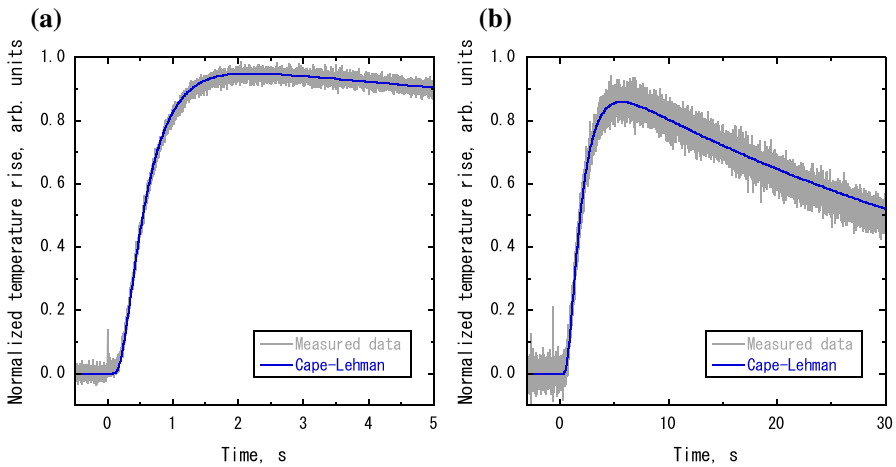


Fig. 4 Temperature change curves of sample YW obtained by laser flash measurements: (a) cross plane (thickness = 1.1 mm); (b) in plane (thickness = 2.5 mm)

Figure 4 shows examples of temperature change curve when YW was measured with the laser flash method. The cross-plane thermal diffusivity was measured by the usual procedure using a 10-mm square-plate specimen, whereas the in-plane thermal diffusivity was measured using the bundled specimens. Figure 4 shows that similar temperature change curves were obtained in both cases. These curves were analyzed using the Cape–Lehman equation corrected by Josell [21,22] and the equiareal method [25]. The temperature change curves were recorded for different intensities of the pulsed laser beam, and the thermal diffusivity was determined according to the procedure given in Akoshima et al. [27] to obtain the intrinsic thermal diffusivity [27].

Figure 5 shows the cross-plane thermal diffusivity α_{cross} and the in-plane thermal diffusivity α_{in} of each TC at room temperature (roughly 23 °C) in air. The thermal

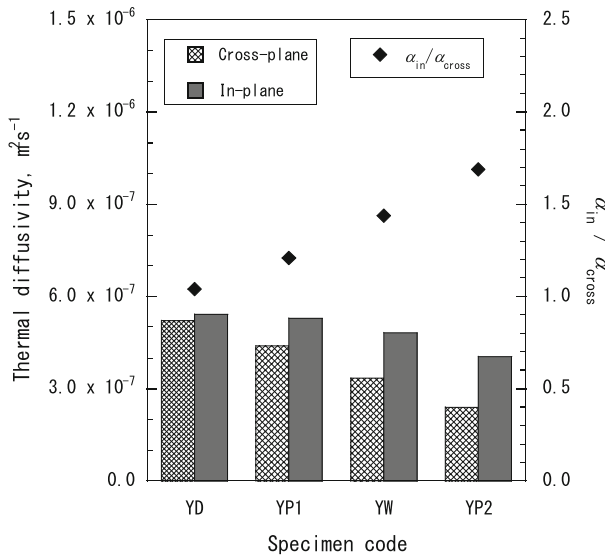


Fig. 5 Cross-plane and in-plane thermal diffusivities of various TCs at room temperature in air

diffusivity ratio $\alpha_{\text{in}}/\alpha_{\text{cross}}$ is also plotted in Fig. 5. Note that we expect an uncertainty of roughly 10% in thermal diffusivity due to measurement uncertainty and the inhomogeneity of the specimens. We judge there to be a significant difference between α_{cross} and α_{in} if $\alpha_{\text{in}}/\alpha_{\text{cross}}$ is greater than 1.10. The general view is that sample YD has isotropic thermal diffusivity because it yields $\alpha_{\text{in}}/\alpha_{\text{cross}} = 1.04$. This view is reasonable from the perspectives of the microstructure shown in Fig. 2 and the porosities shown in Fig. 3. Sample YP1 has small anisotropy in its thermal diffusivity according to its ratio $\alpha_{\text{in}}/\alpha_{\text{cross}} = 1.21$. Although the globular porosities of sample YP1 are almost the same, its cross-plane lamellar porosity is a little higher than its in-plane linear porosity. For sample YW, the thermal diffusivity anisotropy is clear because of its ratio $\alpha_{\text{in}}/\alpha_{\text{cross}} = 1.44$. Its cross-plane total porosity is higher than its in-plane one, as shown in Fig. 3. Its cross-plane lamellar porosity is also higher than its in-plane linear porosity, whereas its globular porosities show no clear difference. Sample YP2 shows the lowest thermal diffusivities among these four types of TC. In fact, its total, globular, lamellar, and linear porosities are the highest among these TCs in both the cross-plane and in-plane views, as shown in Fig. 3. The thermal diffusivity of sample YP2 is especially anisotropic according to its ratio $\alpha_{\text{in}}/\alpha_{\text{cross}} = 1.69$. Its cross-plane total and globular porosities are clearly higher than its in-plane ones.

The cross-plane thermal diffusivity of these four types of TC differs significantly, as shown in Fig. 5. The cross-plane thermal diffusivity ranks as $\text{YW} < \text{YP1} < \text{YD}$. The lamellar porosities are different, although samples YD, YP1, and YW show almost the same cross-plane globular porosity as shown in Fig. 3. There seems to be more lamellar pores in the cross-plane view of sample YP1 compared with sample YD from Fig. 2. It is also evident from Fig. 2 that sample YW has more long lamellar pores compared with sample YP1. We found that the cross-plane thermal diffusivity is sensitive to the lamellar pores. Sample YP2 has large pores and many lamellar pores. The porosities

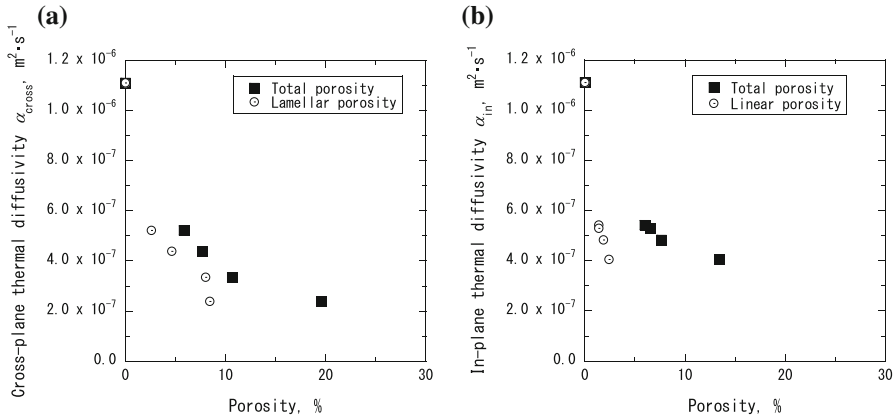


Fig. 6 Dependence of thermal diffusivity on total and lamellar porosity: (a) cross plane; (b) in plane. All measurements taken at room temperature in air

of sample YP2 are the highest among the TCs, and its cross-plane thermal diffusivity is reasonably the lowest among them.

The in-plane thermal diffusivity of sample YP1 is almost the same as that for sample YD, as shown in Fig. 5. The in-plane thermal diffusivity of sample YW is a little lower than those of samples YD and YP1. The in-plane thermal diffusivity difference among these three TCs is very low compared with the cross-plane one. Although the total porosities are almost same, the linear porosity of sample YW is higher than those of samples YD and YP1. The in-plane thermal diffusivity of sample YP2 is lower than that of sample YW. However, the in-plane total and lamellar porosities of sample YP2 are higher than those of sample YW. This indicates that the difference in linear porosity does not have a significant influence in the in-plane TC configuration. These results are reasonable because a coating formed by thermal spraying consists of a lamella of pancake-like particles. We found that the cross-plane thermal diffusivity is readily affected by the microstructure. In particular, we highlight the effect of lamellar pores in decreasing the cross-plane thermal diffusivity. We also found that the in-plane thermal diffusivity is insensitive to changes in the microstructure, unlike the cross-plane one.

To investigate the relationship between thermal diffusivity and microstructure, we plot the thermal diffusivity as a function of porosity in Fig. 6 together with the measured thermal diffusivity of a sintered YSZ specimen. In each case, the thermal diffusivity decreases gradually with total porosity. The total porosity dependence of cross-plane thermal diffusivity is stronger than that of in-plane thermal diffusivity. The cross-plane and in-plane thermal diffusivities decrease specifically with increasing lamellar and linear porosities. However, we found no dependence on globular porosity for either cross-plane or in-plane thermal diffusivity.

We consider linear-shaped pores to be effective for decreasing thermal diffusivity. Similar behavior has been reported recently [28], in which the porosity dependence of thermal conductivity changed according to the pore aspect ratio. There, the cross-plane thermal conductivity showed a large decrease at low porosities when the shape changed from globular to linear [28]. Hence, our results are reasonable according to

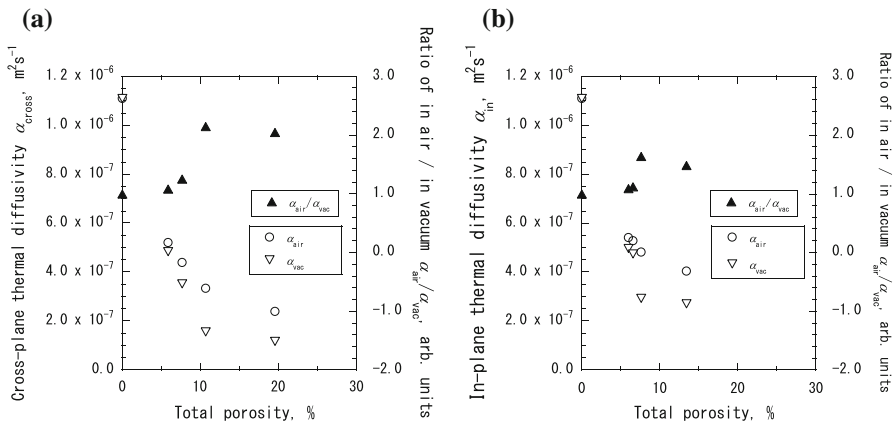


Fig. 7 Dependence of thermal diffusivity on total porosity in air and under vacuum: (a) cross plane; (b) in plane. All measurements taken at room temperature

Ref. [28]. Here, we expect thermal diffusivity to show similar behavior to thermal conductivity because of the thermal transport properties. Our results indicate that the existence of lamellar pores is an effective reason for the observed decrease in the cross-plane thermal diffusivity of the TC.

Figure 7 shows the total porosity dependence of cross-plane and in-plane thermal diffusivities measured in air and under vacuum (~ 1 Pa). The ratios of thermal diffusivity in air and under vacuum are also plotted. We found the thermal diffusivity measured in air to be higher than that measured under vacuum. This is because gas in the pores works as a conductor of heat when the thermal diffusivity of a porous material is measured in a gaseous atmosphere. Therefore, the thermal diffusivity measured in gas should be viewed strictly as the effective thermal diffusivity. The difference in thermal diffusivity between air and vacuum depends on the porosity, as shown in Fig. 7. We expect the comparison between thermal diffusivity in air and under vacuum to give information about the open porosity of the TC. The ratio of thermal diffusivity, $\alpha_{\text{air}}/\alpha_{\text{vac}}$, increases with porosity. It should be noted that the anisotropy of thermal diffusivity measured under vacuum appears similar to that measured in air. The cross-plane and in-plane thermal diffusivities measured under vacuum indicate thermal diffusion phenomena in the microstructure without the influence of gas. The TC has a laminate structure consisting of pancake-like particles, and its microstructure is anisotropic. It is clearly found that the thermal diffusivity of the TC has significant anisotropy according to its anisotropic structure. Therefore, it is important to evaluate both the cross-plane and in-plane thermal diffusivities.

4 Conclusion

We developed a method for measuring the in-plane thermal diffusivity of a TC and studied the thermal diffusivities of TCs formed by thermal spraying under different conditions. The cross-plane thermal diffusivities were measured by the usual laser flash method. The in-plane thermal diffusivities were measured successfully with a

original ceramic jig by the laser flash method. The main results obtained in this study are as follows.

- (1) Plasma-sprayed TCs had significantly anisotropic thermal diffusivities according to their microstructures. The ratio of in-plane thermal diffusivity to cross-plane thermal diffusivity varied from 1.04 to 1.69 in air, and this anisotropy remained even under vacuum.
- (2) Both thermal diffusivities were strongly dependent on the TC porosities. The TC that had large globular pores, many lamellar pores, and many linear pores showed the lowest thermal diffusivity. However, that TC also exhibited more significant anisotropy of its thermal diffusivity.
- (3) Lamellar pores (cracks) in the cross-plane view were effective for decreasing the cross-plane thermal diffusivity of the TC. In contrast, the in-plane thermal diffusivity was insensitive to changes in the in-plane linear porosity.
- (4) It is important to evaluate the anisotropy of the thermal conduction and microstructure of the TC in the thermal design of advanced gas turbines.

Acknowledgements This study was supported financially by the Ministry of Economy, Trade and Industry (METI) of Japan. Part of this work was supported by JSPS KAKENHI Grant Number 15K06490. The authors thank Mr. Yoshihiro Kobayashi, who has graduated the master's course at the Tokyo Metropolitan University graduate school for his contribution in analyzing the TC cross sections.

References

1. X.Q. Cao, R. Vassen, D. Stoeber, J. Eur. Ceram. Soc. **24**, 1–10 (2004)
2. K.E. Wilkes and J.F. Lagedrost, Thermophysical properties of plasma sprayed coatings. NASA Report NASA-CR-121144 (1973)
3. R. Brandt, L. Pawlowski, G. Neuer, High-Temp. High-Press. **18**, 65–77 (1986)
4. R.E. Taylor, Mater. Sci. Eng. A **245**, 160–167 (1998)
5. F. Cernuschi, P. Bianchi, M. Leoni, P. Scardi, J. Therm. Spray Technol. **8**, 102–109 (1999)
6. N. Markocsan, P. Nylén, J. Wigren, X.-H. Li, J. Therm. Spray Technol. **16**, 498–505 (2007)
7. J. Hartman, O. Nilsson, J. Fricke, High-Temp. High Press. **25**, 403–410 (1993)
8. M. Akoshima, T. Tanaka, S. Endo, T. Baba, Y. Harada, Y. Kojima, A. Kawasaki, F. Ono, Jpn. J. Appl. Phys. **50**, 11RE01 (2011)
9. K.B. Larson, Karl Koyama, J. Appl. Phys. **39**, 4408–4416 (1968)
10. H.J. Lee, R.E. Taylor, Therm. Conduct. **14**, 423–434 (1976)
11. N. Araki, A. Makino, T. Ishiguro, J. Mihara, Int. J. Thermophys. **13**, 515–538 (1992)
12. T. Baba, Jpn. J. Appl. Phys. **48**, 05EB04 (2009)
13. N. Takayama, K. Hosono, in *Proceedings of 17th Japan Symposium on Thermophysical Properties* (1996) 375–377 [in Japanese]
14. ISO 18555:2016, Metallic and other inorganic coatings—Determination of thermal conductivity of thermal barrier coatings (2016)
15. A.H. Rossette et al., Appl. Therm. Eng. **29**, 3056 (2009)
16. M. Ogawa, Netsu Bussei **21**, 8–13 (2007). [in Japanese]
17. S. Takahashi, M. Akoshima, T. Tanaka, M. Ogawa, N. Oikawa, Netsu Bussei **30**, 176–181 (2016). [in Japanese]
18. W.J. Parker, R.J. Jenkins, C.P. Butler, G.L. Abbott, J. Appl. Phys. **32**, 1679 (1961)
19. R. Cowan, J. Appl. Phys. **34–4**, 926–927 (1963)
20. D.A. Watt, Brit. J. Appl. Phys. **17**, 231–240 (1966)
21. J.A. Cape, G.W. Lehman, J. Appl. Phys. **34–7**, 1909–1913 (1963)
22. D. Josell, J. Warren, A. Cezairliyan, J. Appl. Phys. **78–11**, 6867–6869 (1995)
23. T. Azumi, Y. Takahashi, Rev. Sci. Instrum. **52**, 1411–1413 (1981)
24. A.B. Donaldson, R.E. Taylor, J. Appl. Phys. **46**, 4584–4589 (1975)

25. ISO 18755:2005, Fine ceramics (advanced ceramics, advanced technical ceramics)—Determination of thermal diffusivity of monolithic ceramics by laser flash method (2005)
26. P. Ctibor, O. Roussel, A. Tricoire, *J. Eur. Ceram. Soc.* **23**, 2993–3999 (2003)
27. M. Akoshima, B. Hay, M. Neda, M. Grelard, *Int. J. Thermophys.* **34**, 778–791 (2013)
28. R. Dutton, R. Wheeler, K.S. Ravichandran, *K. An, J. Therm. Spray Technol.* **9**, 204–209 (2000)